Mol Neurobiol (2017) 54:7620–7638
DOI 10.1007/s12035-016-0232-5

Ovariectomy-Induced Mitochondrial Oxidative Stress, Apoptosis, and Calcium Ion Influx Through TRPA1, TRPM2, and TRPV1 Are Prevented by 17β-Estradiol, Tamoxifen, and Raloxifene in the Hippocampus and Dorsal Root Ganglion of Rats

Yener Yazğan[1] · **Mustafa Nazıroğlu**[1,2,3]

Received: 19 August 2016 / Accepted: 16 October 2016 / Published online: 10 November 2016

Abstract Relative 17β-estradiol (E2) deprivation and excessive production of mitochondrial oxygen free radicals (OFRs) with a high amount of Ca^{2+} influx TRPA1, TRPM2, and TRPV1 activity is one of the main causes of neurodegenerative disease in postmenopausal women. In addition to the roles of tamoxifen (TMX) and raloxifene (RLX) in cancer and bone loss treatments, regulator roles in Ca^{2+} influx and mitochondrial oxidative stress in neurons have not been reported. The aim of this study was to evaluate whether TMX and RLX interactions with TRPA1, TRPM2, and TRPV1 in primary hippocampal (HPC) and dorsal root ganglion (DRG) neuron cultures of ovariectomized (OVX) rats. Forty female rats were divided into five groups: a control group, an OVX group, an OVX+E2 group, an OVX+TMX group, and an OVX+RLX group. The OVX+E2, OVX+TMX, and OVX+RLX groups received E2, TMX, and RLX, respectively, for 14 days after the ovariectomy. E2, ovariectomy-induced TRPA1, TRPM2, and TRPV1 current densities, as well as accumulation of cytosolic free Ca^{2+} in the neurons, were returned to the control levels by E2, TMX, and RLX treatments. In addition, E2, TMX, and RLX via modulation of TRPM2 and TRPV1 activity reduced ovariectomy-induced mitochondrial membrane depolarization, apoptosis, and cytosolic OFR production. TRPM2, TRPV1, PARP, and caspase-3 and caspase-9 expressions were also decreased in the neurons by the E2, TMX, and RLX treatments. In conclusion, we first reported the molecular effects of E2, TMX, and RLX on TRPA1, TRPM2, and TRPV1 channel activation in the OVX rats. In addition, we observed neuroprotective effects of E2, RLX, and TMX on oxidative and apoptotic injuries of the hippocampus and peripheral pain sensory neurons (DRGs) in the OVX rats.

Keywords Hippocampus · Ovariectomy · Raloxifene · Tamoxifen · TRPM2 · TRPV1

Abbreviations

$[Ca^{2+}]_i$	Cytosolic free calcium ion
ACA	N-(p-Amylcinnamoyl) anthranilic acid
ADPR	ADP-ribose
CAP	Capsaicin
CHPx	Cumene hydroperoxide
CPZ	Capsazepine
DMSO	Dimethyl sulfoxide
DRG	Dorsal root ganglion
E2	17β-Estradiol
EGTA	Ethylene glycol-bis[2-aminoethyl-ether]-*N*,*N*,*N*,*N*-tetraacetic acid
HPC	Hippocampal
MPT	Permeability transition
OFR	Oxygen free radials
PARP	Poly(ADP-ribose) polymerase
RLX	Raloxifene
TMX	Tamoxifen
TRP	Transient receptor potential
TRPA1	Transient receptor potential ankyrin 1
TRPM2	Transient receptor potential melastatin
TRPV1	Transient receptor potential vanilloid 1

✉ Mustafa Nazıroğlu
mustafanaziroglu@sdu.edu.tr

[1] Department of Biophysics, Institute of Health Science, Suleyman Demirel University, Isparta, Turkey

[2] Neuroscience Research Center, University of Suleyman Demirel, Isparta, Turkey

[3] Nörolojik Bilimler Uygulama ve Araştırma Merkezi Müdürü, Süleyman Demirel Üniversitesi, TR 32260 Isparta, Turkey

VGCC Voltage-gated calcium channels
WC Whole cell

Introduction

Transient receptor potential (TRP) family with eight subfamily cation channels is the Ca^{2+}-permeable and potential drug discovery cation channels although they have been discovered as cation channels within last decades. A member of TRP family in melastatin group is TRP melastatin 2 (TRPM2). Secondary products of many physiological functions, such as mitochondria function and phagocytosis, are production oxygen free radicals (OFRs) [1, 2]. The N domain of TRPM2 channel contains the ADP-ribose (ADPR) pyrophosphate enzyme. Separately, activation of the enzyme by ADPR and OFR were discovered within the last decade [3, 4]. TRP vanilloid 1 (TRPV1) is another member of the TRP family, which is activated by different stimuli, including the main component in hot chili peppers (capsaicin) [5–7]. Cysteine groups are main target of oxidative stress in cellular membranes, and TRPV1 and TRP ankyrin 1 (TRPA1) have rich content of cysteine groups in its structure [8]. Hence, TRPV1 and TRPA1 is also oxidative stress-sensitive Ca^{2+}-permeable channels. Therefore, activation of TRPA1 in cells by H_2O_2 was reported [9]. The TRPA1, TRPM2, and TRPV1 play an important role in the pain transmission of sensory neurons, including the dorsal root ganglion (DRG), and in injury of certain brain regions, including the hippocampus [10–12]. The expression levels of TRPA1, TRPM2, and TRPV1 are highest in the DRG and hippocampal (HPC) neurons [5, 13–16]. The channels in the DRG and the hippocampus are potential new targets through TRPA1, TRPM2, and TRPV1 inhibition for the management of pain and oxidative brain injury [12, 16, 17]. Recently, decreased TRPV1 expression levels have been reported in the DRG of 17β-estradiol (E2) receptors of knockout mice [18]. In addition, interaction between E2 treatment and HPC neuron TRPV1 has been reported in ovariectomized (OVX) rats [10]. Hence, E2 may also play a key role in interacting with Ca^{2+} in pain modulation and HPC neuron injury inhibition by inhibiting TRPM2 and TRPV1 activation.

Tamoxifen (TMX) and raloxifene (RLX) are selective E2 receptor modulators (SERMs) in menopause that are used for the treatment of breast cancer and osteoporosis, respectively. TMX is an estrogen antagonist in mammary tissue, but it regulates the effects of estrogen in the brain and neurons [19]. In addition to their anticancer and bone protective effects, TMX and RLX are lipophilic drugs and strong intramembranous OFR scavengers in tissues, including the brain [20–22]. Recent report indicates the neuroprotective and mitochondrial OFR scavenging role of TMX against ischemia [19] and brain oxidative injury [20]. RLX-induced neuroprotective and pain modulator effects through inhibition of the excitotoxic glutamate-induced increase in cytosolic free Ca^{2+} ion concentration ($[Ca^{2+}]_i$) [23] and similar neuroprotective and pain modulator effects may present via TRPM2 and TRPV1.

In addition to energy production, mitochondria play an important role in cell death. It is well known that prolonged changes in Ca^{2+} distribution, including an elevation in mitochondrial membrane depolarization, trigger a variety of cascades that lead to cell death [2]. Recently, we observed protective effects of antioxidants on neuronal toxicity, mitochondrial oxidative stress, and Ca^{2+} influx through modulation of TRPM2 and TRPV1 in the HPC and DRG of rats [11, 12]. TMX and RLX reduced the mitochondrial membrane potential dependent complex III and mitochondrial permeability transition (MPT)-mediated OFR formation [20, 24]. The antioxidants TMX and RLX may reduce oxidative stress, apoptotic factors (including caspase-3 and caspase-9), mitochondrial membrane depolarization, and Ca^{2+} influx through the inhibition of TRPA1, TRPM2, and TRPV1 activation. This effect should be examined in the DRG and hippocampus of OVX-treated rats.

Overload Ca^{2+} influx through voltage-gated calcium channels (VGCCs) and glutamate receptors in the DRG and hippocampus of rats was decreased by RLX and TMX treatments [23, 25]. RLX and TMX may modulate Ca^{2+} influx via TRPA1, TRPM2, and TRPV1, thus affecting oxidative stress and apoptosis in the DRG and hippocampus of rats with OVX-induced brain injury. In the current study, we aimed to investigate the effects of E2, TMX, and RLX treatments on mitochondrial oxidative stress, apoptosis, and Ca^{2+} influx through TRPM2 and TRPV1 in the DRG and HPC of OVX rats.

Materials and Methods

Animals

Forty female Wistar albino rats (3 months old) were housed in the Experimental Animal Research Center of Suleyman Demirel University (SDU). They were kept under controlled light (12 h day/night cycle) and humidity (60 %) with free access to water (except during the fasting period) and commercial feed. Adhering to procedures approved by the Local Experimental Animal Ethical Committee of SDU (potocol number 2015-08), the animals were sacrificed by decapitation.

Study Groups

The 40 rats were randomly divided into five groups, with eight rats per group, as follows:

Control Group A placebo (0.1 ml dimethyl sulfoxide [DMSO] + 0.9 ml physiological saline [0.9 NaCl *w*/*v*]) was subcutaneously administrated to the group for 14 days.

OVX Group OXV was induced, and DMSO was subcutaneously supplemented for 14 days [26].

OVX+E2 Group Animals received subcutaneous E2 (80 μg/kg/day) for 14 consecutive days after OVX treatment [27].

OVX+TMX Group OVX and TMX (1 mg/kg/day) were subcutaneously given for 14 consecutive days [28].

OVX+RLX Group Animals received subcutaneous RLX (1 mg/kg/day) for 14 consecutive days after OVX treatment [21].

Bilateral ovariectomies were performed in all groups except for the control group, as previously described [26, 28]. E2, TMX, and RLX (Cayman Chemical Inc., Istanbul, Turkey) were dissolved in DMSO (0.1 ml).

Preparation of the Brain and Neuron Samples

After 12 h fasting, all rats were decapitated by cervical dislocation in accordance with SDU Experimental Animal legislation. The brain cortex, DRG, and HPC neuronal samples were isolated as described in previous studies [11]. First, hippocampus was taken into Hank's buffered salt solution (HBSS), and then, it was mechanically dissociated by trituration. HPC neurons from the hippocampus were obtained by incubation with trypsin solution for 35 min. The hippocampus in the trypsin solution was also mixed every 10 min for isolation of HPC neurons. For obtaining DRG neurons, the connectives of spinal cord were mechanically cut by a surgical scissor from L4 and L5. Collagenase IV (2 mg/ ml and Worthington Inc., Istanbul, Turkey) and trypsin (2.5 mg/ml and Worthington) were prepared in DMEM, and the ganglia were incubated with the collagenase IV and trypsin in incubator (95 % air, 5 % CO_2) for 45 min at 37 °C. For obtaining medium and big size DRGs, we used a sterile syringe with different tips. After centrifugation (1000*g* for 10 min), the neurons were taken removed for analysis as described a previous study [11].

Except Western blot analyses, we used life HPC and DRG neurons which were counted by Cell Counter and Analyzer of CASY Model TTC, Roche Diagnostics Corporation, IN, USA). They divided into sections as 1×10^5 cells/ml on sterile culture dishes in the incubator. The HPC and DRG neurons for Western blot analyses were kept at −85 °C for 1 month after washing phosphate buffer (pH 7.2).

Records of Electrophysiology

Whole-cell record mode of patch-clamp technique (EPC10 patch-clamp set, HEKA, Lamprecht, Germany) used in the DRG of current study as described in previous studies [11, 12]. The final resistance of cytosolic solution-filled whole cell recording electrodes was between 2 and 8 MΩ. The borosilicate capillary pipettes were prepared by a puller (pc-10 model, Narishige Inc., Tokyo, Japan). Content and osmolality details of the extracellular patch chamber and patch pipette solutions were given in previous studies [4, 11]. For preparing Na^+-free extracellular solution, 150 mM N-methyl-D-glucamine ($NMDG^+$) instead of instead of NaCl after pH arrangement with HCl was used. It is well known that the TRPM2 is activated by presence of high cytosolic $[Ca^{2+}]_i$ [29]. Therefore, intracellular buffer calcium contents of the buffers were prepared 1 μM instead of 0.08 μM. Calculation of the Ca^{2+} concentrations in the solutions were performed by a specific program as described previous studies [11, 12].

In the patch-clamp analyses of the DRG neurons, −60 mV was the holding potential. We used voltage clamp instead of current clamp in the analyses, and we recorded current changes. Current and voltage (*I-V*) relationships were obtained from voltage ramps from −90 to +60 mV applied over 400 ms. All experiments were done at room temperature (22 ± 1 °C). For the analysis, the maximal current amplitudes (pA) in a DRG neuron were divided by the cell capacitance (pF), a measure of the cell surface. The current density (pA/pF) was used as unit of the TRPA1, TRPM2 and TRPV1 activations in the neuron.

Preparation Agonist and Antagonists of TRPA1, TRPM2 and TRPV1 Channels

Stock solution of the agonists and antagonists were prepared in DMSO. ADPR was diluted to reach the therapeutic concentrations by extracellular solution although remaining agonists and antagonists were diluted by extracellular solutions. In the patch-clamp experiments, agonist and antagonist of TRPM2 were H_2O_2 (10 mM) and antralic acid N-(p-amylcinnamoyl) anthranilic acid (ACA, 0.025 mM) in patch chamber, respectively. TRPV1 was gated by adding extracellular capsaicin (CAP, 0.010 mM), and the channels were inhibited administration of capsazepine (CPZ, 0.1 mM) into patch chamber. TRPA1 was gated by adding extracellular H_2O_2 (10 mM), and the channel was inhibited administration of AP18 (0.02 mM) into patch chamber.

Measurement of $[Ca^{2+}]_i$ Concentration

Fura-2 acetoxymethyl ester (fura-2AM) is a high affinity, cytosolic Ca^{2+} indicator that is UV light-excitable [2]. The neurons were incubated in serum-free media with 5 μM fura-2AM for 40 min according to a procedure described elsewhere [2, 11, 12]. Then, the neurons were washed twice with 20 mM HEPES solution (pH 7.4) by centrifugation at 2500*g* for 5 min to remove the free dye and resuspended in the same buffer. In TRPM2 experiments, channels were immediately stimulated

by cumene hydroperoxide (CHPx) after incubation of ACA (0.025 mM) for 10 min. In TRPV1 experiments, the neurons were immediately stimulated by capsaicin after incubation of CPZ (0.1 mM) for 30 min. Fluorescence of magnetically stirred neuronal suspension (1 mg protein) was adjusted to an excitation wavelength of 340 and 380 nm, emission wavelength of 505 nm in a spectrofluorometer (Carry Eclipsys, Varian Inc., Sydney, Australia). The Fura 2-AM 340/380 nm fluorescence ratio is used as indicator of the in $[Ca^{2+}]_i$ concentration in a computer and calibration of the ratio were performed by the method of Grynkiewicz et al. [30].

Cytosolic OFR Production Measurement

Rhodamine 123 (Rh123) is a green-fluorescent dye which locates in the mitochondria of cells. Once getting in the HPC and DRG neurons, DHR 123 becomes fluorescent upon oxidation to Rh123 and the fluorescence

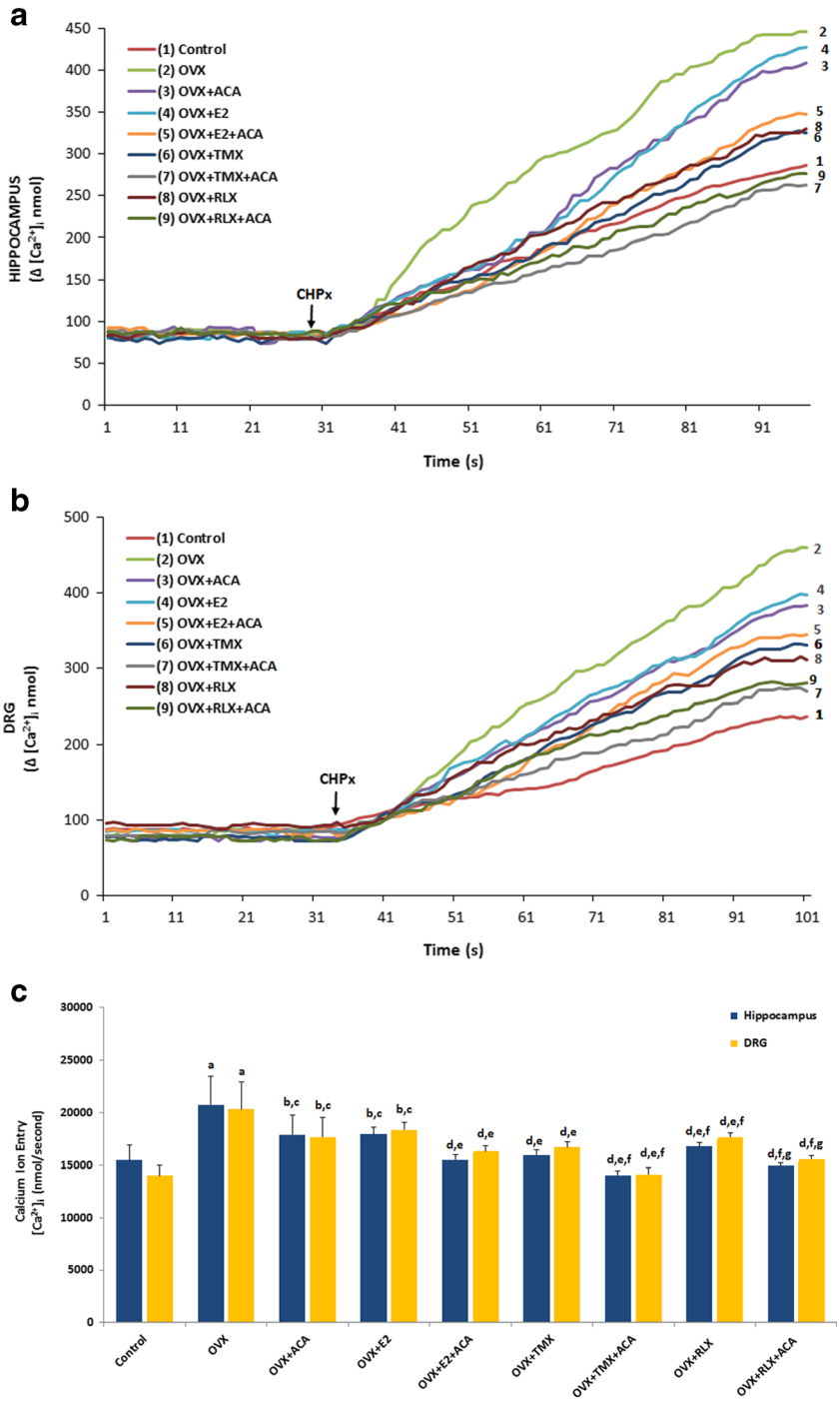

Fig. 1 Roles of E2, TMX, and RLX treatments on $[Ca^{2+}]_i$ through TRPM2 in HPC (**a**)and DRG (**b**) neurons in control and OVX rats ($n = 8$ and mean ± SD). The animals in the E2, TMX, and RLX groups subcutaneously received 80, 1, and 1 mg/kg after ovariectomy, respectively. HPC and DRG neurons were dissected from control and treated animals, and they were further treated with the TRPM2 agonist cumene hydroperoxide (CHPx, 1 mM) for 99 or 101 s. The TRPM2 in the neurons were inhibited by ACA (0.025 mM) ($^{a}p < 0.001$ and $^{b}p < 0.05$ versus control group, $^{c}p < 0.05$ and $^{e}p < 0.001$ versus OVX group, $^{d}p < 0.05$ versus OVX+E2 group, $^{f}p < 0.05$ versus OVX+TMX group, $^{g}p < 0.05$ versus OVX+RLX group) (**c**)

indicates proportional ratio of OFR generation changes. The DRG and HPC neurons were incubated with 20 μm DHR 123 for 25 min [31]. The fluorescence intensity of Rh123 was measured in the neurons by an automatic microplate reader (Infinite pro200; Tecan Austria GmbH, Groedig, Austria). Excitation was set at 488 nm and emission at 543 nm. The data are presented as fold increase over the pretreatment level.

Determination of Mitochondrial Membrane Potential (JC-1)

The mitochondrial membrane potential (JC-1) was determined by JC-1 dye as described in previous studies [2, 11, 31]. In health cells, the dye concentrates in the mitochondrial matrix, where it forms red fluorescent aggregates (J-aggregates), and the dye is dispersed throughout the entire cell

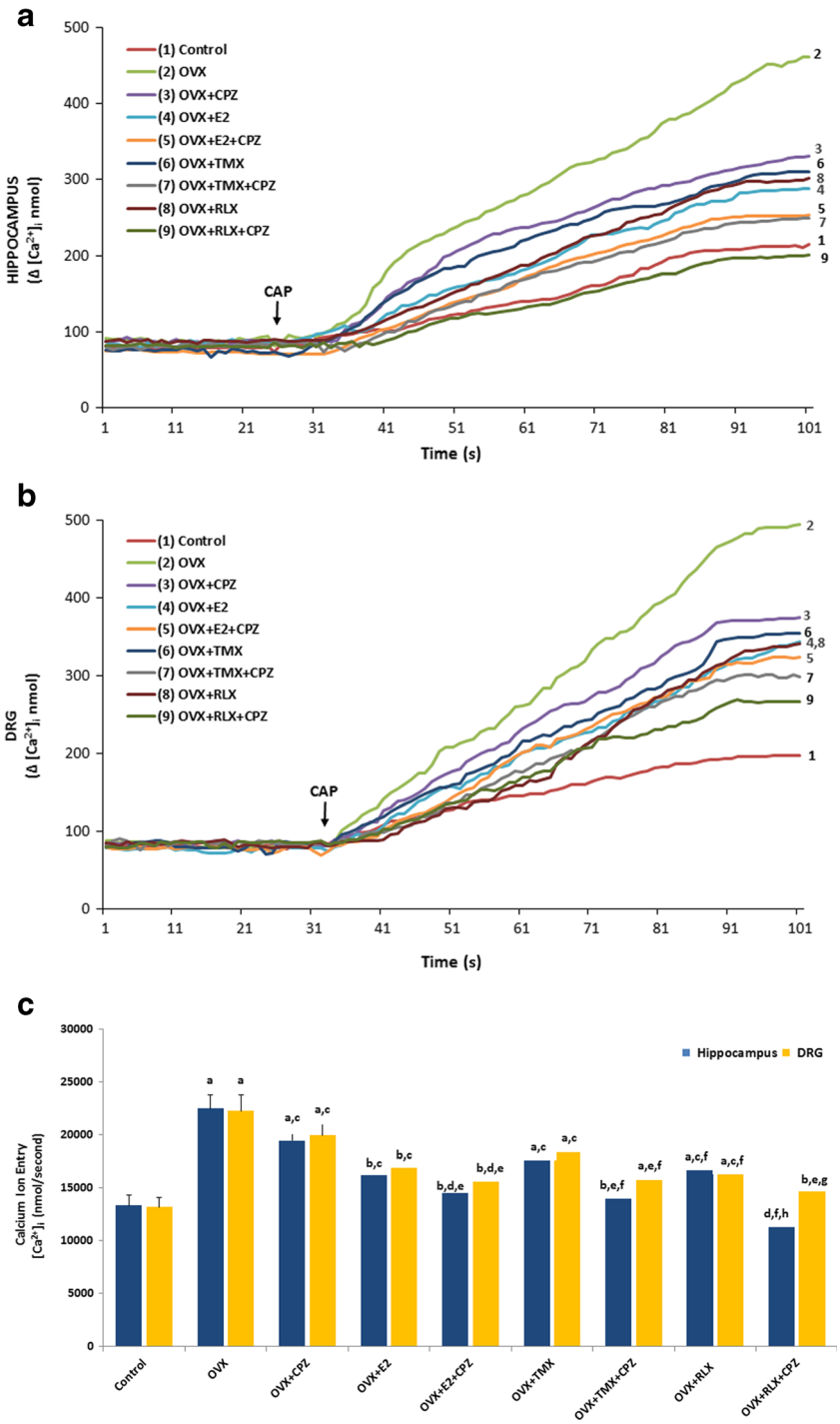

Fig. 2 Roles of E2, TMX, and RLX treatments on $[Ca^{2+}]_i$ through TRPV1 in HPC (**a**) and DRG (**b**) neurons in control and OVX rats ($n = 8$ and mean ± SD). The animals in the E2, TMX, and RLX groups subcutaneously received 80, 1, and 1 mg/kg after ovariectomy, respectively. Dissected HPC and DRG were neurons were further treated with the TRPV1 agonist capsaicin (CAP and 0.01 mM) in the presence of normal extracellular calcium (1.2 mM) for 99 to 101 s. The TRPV1 in the neurons was inhibited by capsazepine (CPZ and 0.1 mM) ($^{a}p < 0.001$ and $^{b}p < 0.05$ versus control group, $^{c}p < 0.05$ and $^{c}p < 0.001$ versus OVX group, $^{d}p < 0.05$ versus OVX+E2 group, $^{f}p < 0.05$ versus OVX+TMX group, $^{g}p < 0.05$ and $^{h}p < 0.001$ versus OVX+RLX group) (**c**)

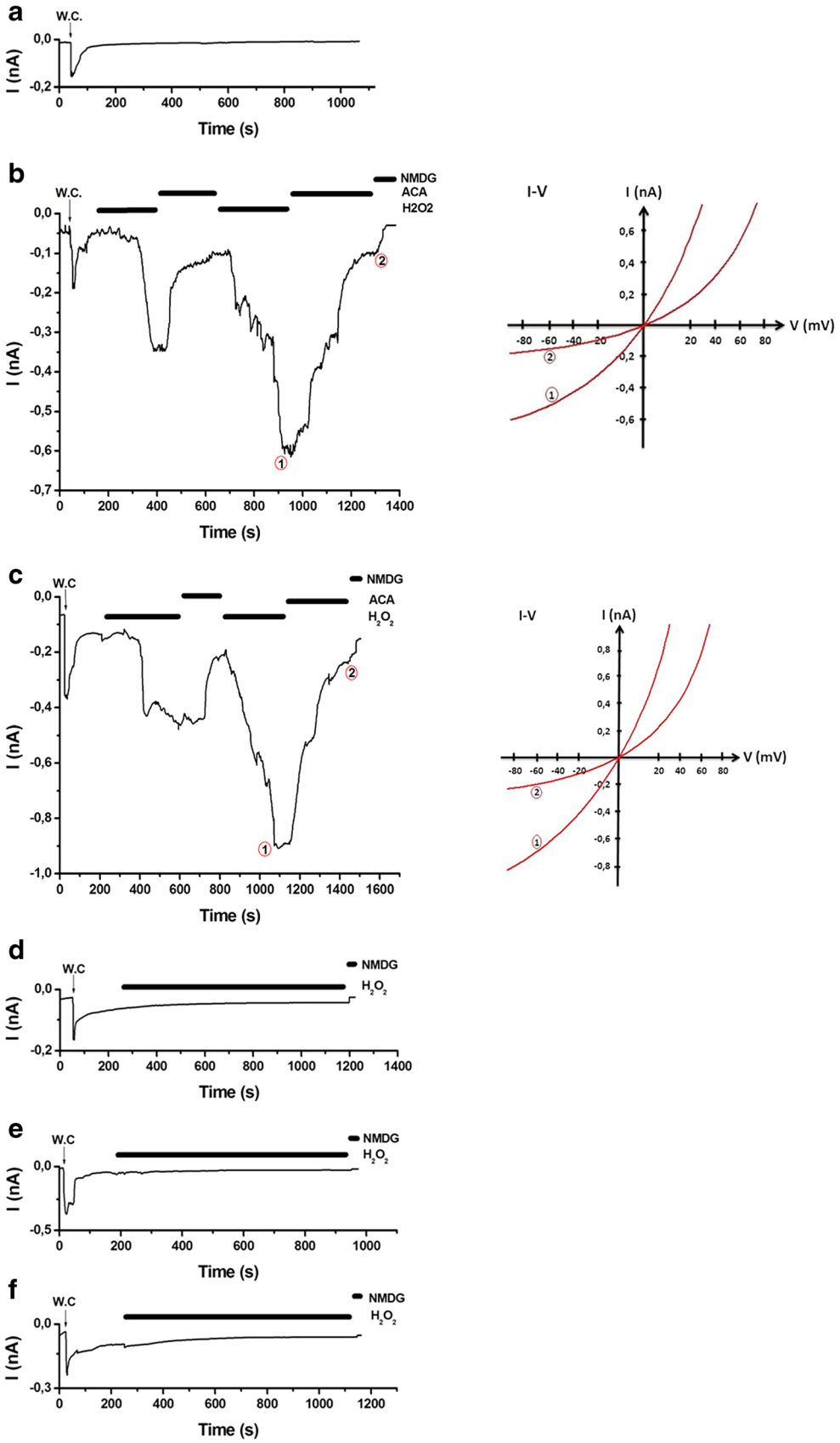
a
W.C.
I (nA)
Time (s)
b
W.C.
NMDG
ACA
H2O2
I (nA)
Time (s)
I-V
I (nA)
V (mV)
c
W.C
NMDG
ACA
H2O2
I (nA)
Time (s)
I-V
I (nA)
V (mV)
d
W.C
NMDG
H2O2
I (nA)
Time (s)
e
W.C
NMDG
H2O2
I (nA)
Time (s)
f
W.C
NMDG
H2O2
I (nA)
Time (s)

◀ **Fig. 3** Effects of E2, TMX, and RLX treatments on TRPM2 activation in the DRG of control and OVX rats. The holding potential of whole-cell (WC) records was −60 mV. **a** Control: Records from control neuron without stimulation of H_2O_2. **b** Control+H_2O_2 group: DRG was isolated from rats of the control group without ovariectomy induction and activated in the patch chamber by extracellular H_2O_2 (10 mM), and it was blocked by ACA (0.025 mM). **c** OVX group: TRPM2 currents in the DRG neurons of OVX rats were gated by H_2O_2 (10 mM) in the patch chamber, and they were inhibited by ACA (0.025 mM) in the bath of the patch chamber. **d**, **e**, and **f** groups: The rats subcutaneously received E2, TMX, and RLX after ovariectomy, respectively; then, the DRG neurons were stimulated by in vivo H_2O_2 (10 mM)

leading to a shift from red (J-aggregates) to green fluorescence (JC-1 monomers). The neurons were incubated with JC-1 at 37 °C for 45 min. JC-1-loaded cells were excited at 488 nm, and emission was detected at 590 nm (JC-1 aggregates) and 525 nm (JC-1 monomers). Values were calculated from emission ratios (590/525). The data are presented as fold increase over the pretreatment level.

Assay for Apoptosis, Caspase-3, and Caspase-9 Activities

The apoptosis assay was performed in spectrophotometer (UV-1800 Shimadzu, Kyoto, Japan) by using a commercial kit according to the instructions provided by Biocolor Ltd. (Northern Ireland) and elsewhere [11].

The determinations of caspase-3 and caspase-9 activities in the HPC and DRG neurons were performed in the microplate reader (Infinite pro200) by using caspase-3 (N-acetyl-Asp-Glu-Val-Asp-7-amino-4-methylcoumarin) and caspase-9 (His-Asp-7-amino-4-methylcoumarin) substrates. Buffer and chemical details on the determinations of caspase-3 and caspase-9 activities in HPC and DRG were based on methods previously reported [11]. The substrate cleavage was measured at 360 nm (excitation) and 460 nm (emission). Values were calculated as fluorescence units/mg protein, and caspase-3 and caspase-9 activities were expressed as fold increase.

Analyses of Western Blot and Channel Expression

All Western blot analyses in the brain were performed using standard procedures [11]. To detection of TRPM2 and TRPV1 cation channels, procaspase-3, procaspase-9, and poly-ADP-ribose polymerase 1 (PARP1) expression levels, cells were homogenized in lyses buffer, the supernatants removed and conserved after centrifuged at 16,000*g* for 20 min. After that, the membranes were incubated with primary antibodies, TRPM2 and TRPV1 (anti-TRPM2 antibody and anti-VR1 antibody; Abcam, Cambridge, UK) and others (caspase-9/p35/p10 polyclonal antibody; caspase-3, p17-specific polyclonal antibody; beta-actin polyclonal antibody; PARP1 polyclonal antibody; Proteintech, USA) and secondary antibody (rabbit IgG, HRP-linked whole Ab, from donkey; GE Healthcare, Amersham, UK). Bands were visualized using ECL Western HRP Substrate (Millipore Luminate Forte, USA), and imaging was achieved with (G:Box, Syngene, UK) and normalized against β-actin protein.

Statistical Analyses

All data were represented as means ± standard deviation (SD). The data were analyzed by using 17.0 version of SPSS statistical program (Chicago, IL, USA). $p < 0.05$ was considered to indicate a statistically significant difference. Presence of significance in the five groups was once detected by ANOVA and LSD tests. Then *p* value levels of significances in the data were analyzed by using Mann-Whitney *U* test.

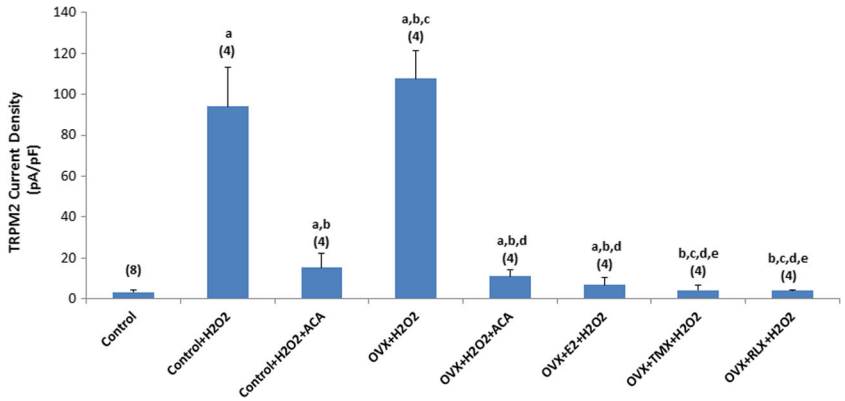

Fig. 4 Protective roles of E2, TMX, and RLX treatments on TRPM2 capacitances of the DRG in control and OVX rats (mean ± SD). The DRG neurons were stimulated in vitro (in the patch chamber) with H_2O_2 (10 mM), although they were inhibited by ACA (0.025 mM). *N* numbers of the groups are indicated in parentheses. Significant stimulation and inhibition of currents are expressed by *letters* ($^a p < 0.001$ versus control, $^b p < 0.001$ versus control+H_2O_2 group, $^c p < 0.001$ versus control+H_2O_2+ACA group, $^d p < 0.001$ versus OVX+H_2O_2 group, $^e p < 0.001$ versus OVX+E2+H_2O_2 group)

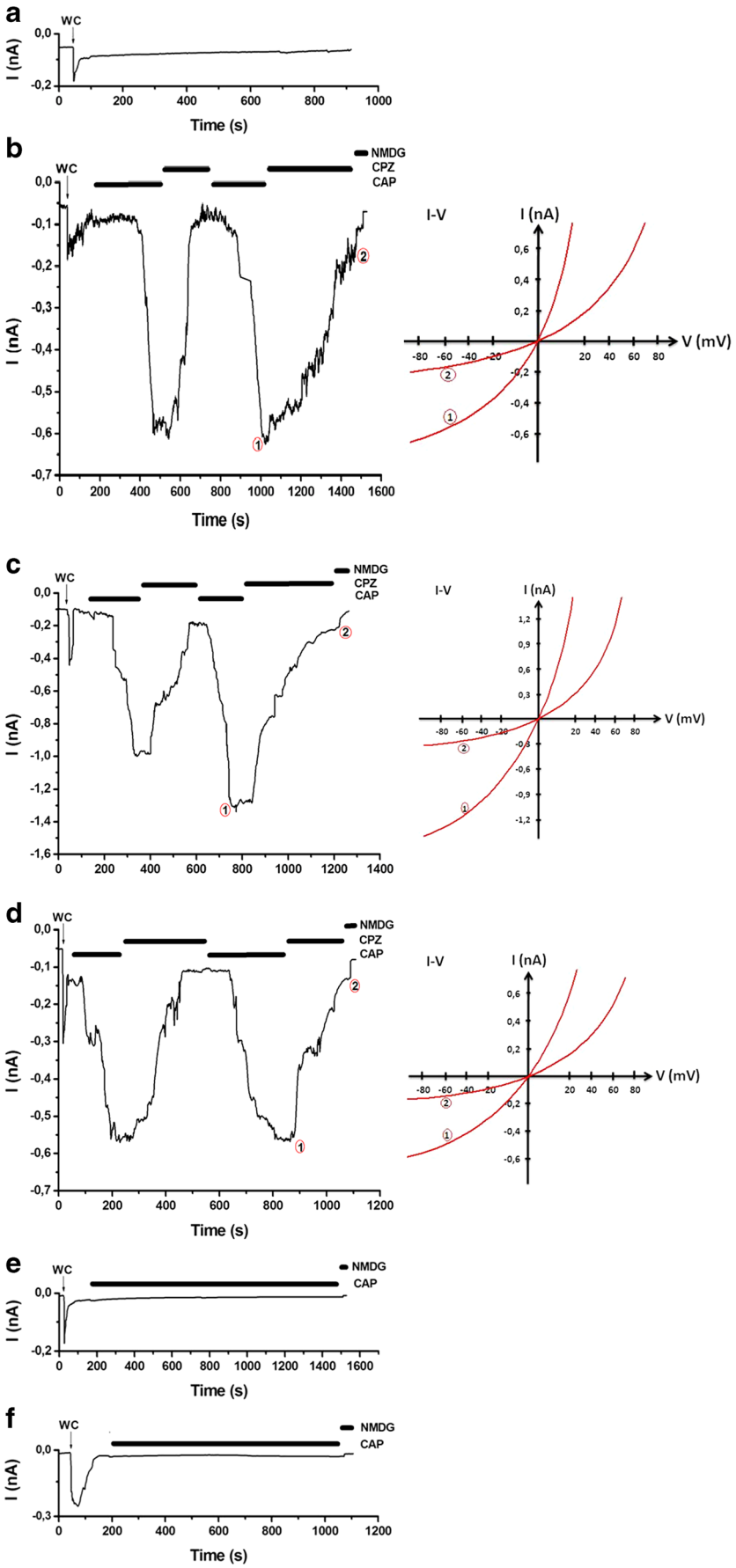

Fig. 5 Effects of E2, TMX, and RLX treatments on TRPV1 in the DRG of control and OVX rats. The holding potential was −60 mV. Except for control records, TRPV1 currents in the DRG neurons of rats were gated by capsaicin (CAP and 0.01 mM) in the patch chamber, and they were inhibited by capsazepine (CPZ and 0.1 mM) in the bath of the patch chamber. **a** Control: Records from the control neuron without stimulation of CAP. **b** Control+CAP group: DRG was isolated from control rats without ovariectomy induction, and then, they were stimulated by CAP but inhibited by CPZ. **c** OVX+CAP group: TRPV1 currents in the DRG neurons of OVX rats were gated by CAP but inhibited by CPZ. **d** OVX+E2 group: The rats received subcutaneous E2 (80 μg/kg) for 14 days after ovariectomy, and then, the DRG neurons were stimulated by CAP but inhibited by CPZ. **e** OVX+TMX group: After treatment of subcutaneous TMX (1 mg/kg) for 14 days in OVX rats, the DRG was stimulated by CAP. **f** OVX+RLX group: After treatment of subcutaneous RLX (1 mg/kg) for 14 days in OVX rats, the DRG was stimulated by CAP. *WC* whole cell

Results

The Protective Roles of E2, TMX, and RLX on Ca^{2+} Influx Through TRPM2 Channels in the Hippocampus and DRG of OVX Rats

There is no specific antagonist of TRPM2, although ACA is the best TRPM2 antagonist among the antagonists [32]. Therefore, we used it to examine the potential therapeutic roles of E2, TMX, and RLX in ovariectomy-induced neuronal injury in the hippocampus and the DRG through TRPM2 involved in Ca^{2+} accumulation. Ca^{2+} influx into HPC and DRG neurons is illustrated in Fig. 1a, b, respectively. Calibration ratio of the cytosolic Ca^{2+} entry as nmol/s in the HPC and DRG are indicated in Fig. 1c. Compared to control, the Ca^{2+} influx into HPC and DRG neurons was significantly ($p < 0.001$) high in the OVX group. Compared to the OVX only group, the Ca^{2+} influx was markedly ($p < 0.05$) low in the OVX+E2, OVX+TMX, and OVX+RLX groups. Compared to the OVX+E2, OVX+TMX, and OVX+RLX groups, the $[Ca^{2+}]_i$ influx was lower ($p < 0.05$) in the OVX+E2+ACA, OVX+TMX+ACA, and OVX+RLX+ACA groups due to the ACA treatments. The $[Ca^{2+}]_i$ accumulation was also lower in the OVX+RLX+ACA group than in the OVX+TMX+ACA and OVX+E2+ACA groups ($p < 0.05$).

The Protective Roles of E2, TMX, and RLX on Ca^{2+} Influx Through TRPV1 in the Hippocampus and DRG of OVX Rats

The best specific TRPV1 antagonist and agonist are CPZ and CAP, respectively [5]. For clarifying the TRPV1 involved in Ca^{2+} accumulation in the HPC and DRG neurons, stimulation of the neurons were performed by extracellular CAP, although their inhibition were performed by CPZ (Fig. 2a–c). The $[Ca^{2+}]_i$ accumulation in the neurons was increased by ovariectomy induction, and it was markedly ($p < 0.001$) higher in the OVX group than in the control group. Compared to the OVX group, Ca^{2+} influx was markedly ($p < 0.05$) lower in the OVX+E2, OVX+TMX, and OVX+RLX groups due to the E2, TMX, and RLX treatments. Compared to the OVX+E2, OVX+TMX, and OVX+RLX groups, the $[Ca^{2+}]_i$ accumulation was further decreased ($p < 0.05$) in the OVX+E2+CPZ, OVX+TMX+CPZ, and OVX+RLX+CPZ groups by CPZ treatments. The $[Ca^{2+}]_i$ accumulation was also lower in the OVX+RLX+CPZ group than in the OVX+TMX+CPZ and OVX+E2+CPZ groups ($p < 0.05$). It seems that the effects of RLX via TRPV1 on $[Ca^{2+}]_i$ accumulation were also highest within the E2, TMX, and RLX-treated groups.

The Protective Roles of E2, TMX, and RLX on TRPM2 Capacitances in the DRG of OVX Rats

TRPM2 is activated either by oxidative stress products or ADPR [4]. TRPM2 channels were activated in a patch-clamp experiment of the current study using H_2O_2 as an oxidative stress product. The H_2O_2 induces air bubbles in the patch pipette. Hence, the H_2O_2 was applied to the DRG neurons through a patch chamber. TRPM2 currents of H_2O_2 in the DRGs were observed between 0.7 and 1.3 min, and reaching amplitudes of the neurons were above 0.55 nA. These currents were returned to the control levels by the ACA and $NMDG^+$ treatments (Fig. 3b, c). We obtained no current in the absence of H_2O_2 (controls) using the DRG of the same animals (Fig. 3a). The mean values of the current densities (in terms of pA/pF) of the DRG neurons were markedly ($p < 0.001$)

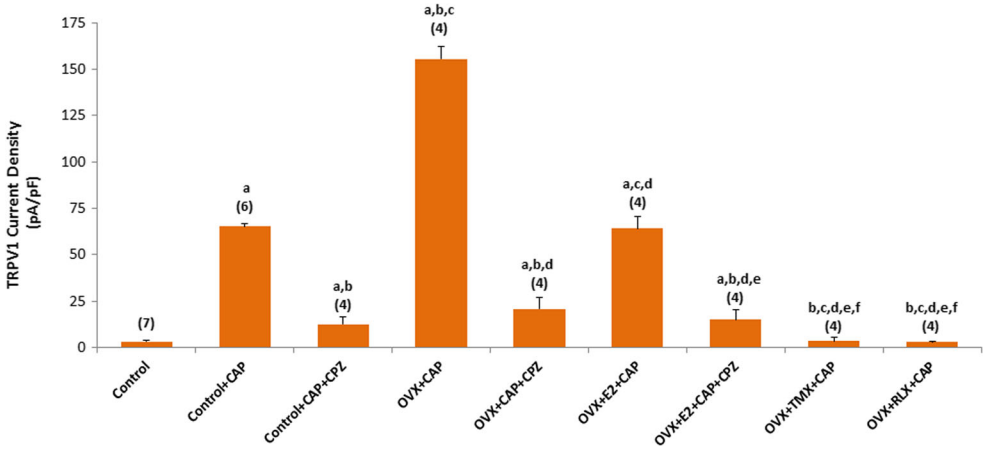

Fig. 6 Protective roles of E2, TMX, and RLX treatments on TRPV1 capacitances of the DRG in control and OVX rats. The DRG neurons were stimulated in vitro (in the patch chamber) with CAP (0.01 mM), although they were inhibited by CPZ (0.1 mM). *N* numbers of the groups were indicated in parentheses ($^a p < 0.001$ versus control, $^b p < 0.001$ versus control+CAP group, $^c p < 0.001$ versus control+CAP+CPZ group, $^d p < 0.001$ versus OVX+CAP group, $^e p < 0.001$ versus OVX+E2+CAP group, $^f p < 0.001$ versus OVX+E2+CAP+CPZ group)

higher in the control+H_2O_2 (94.08 pA/pF) and OVX+H_2O_2 (107.70 pA/pF) groups than in the control group (3.21 pA/pF). In comparison to the control+H_2O_2 group, the densities were further increased in the OVX+H_2O_2 group by ovariectomy induction. However, the mean current densities were decreased to control levels in the control+H_2O_2+ACA

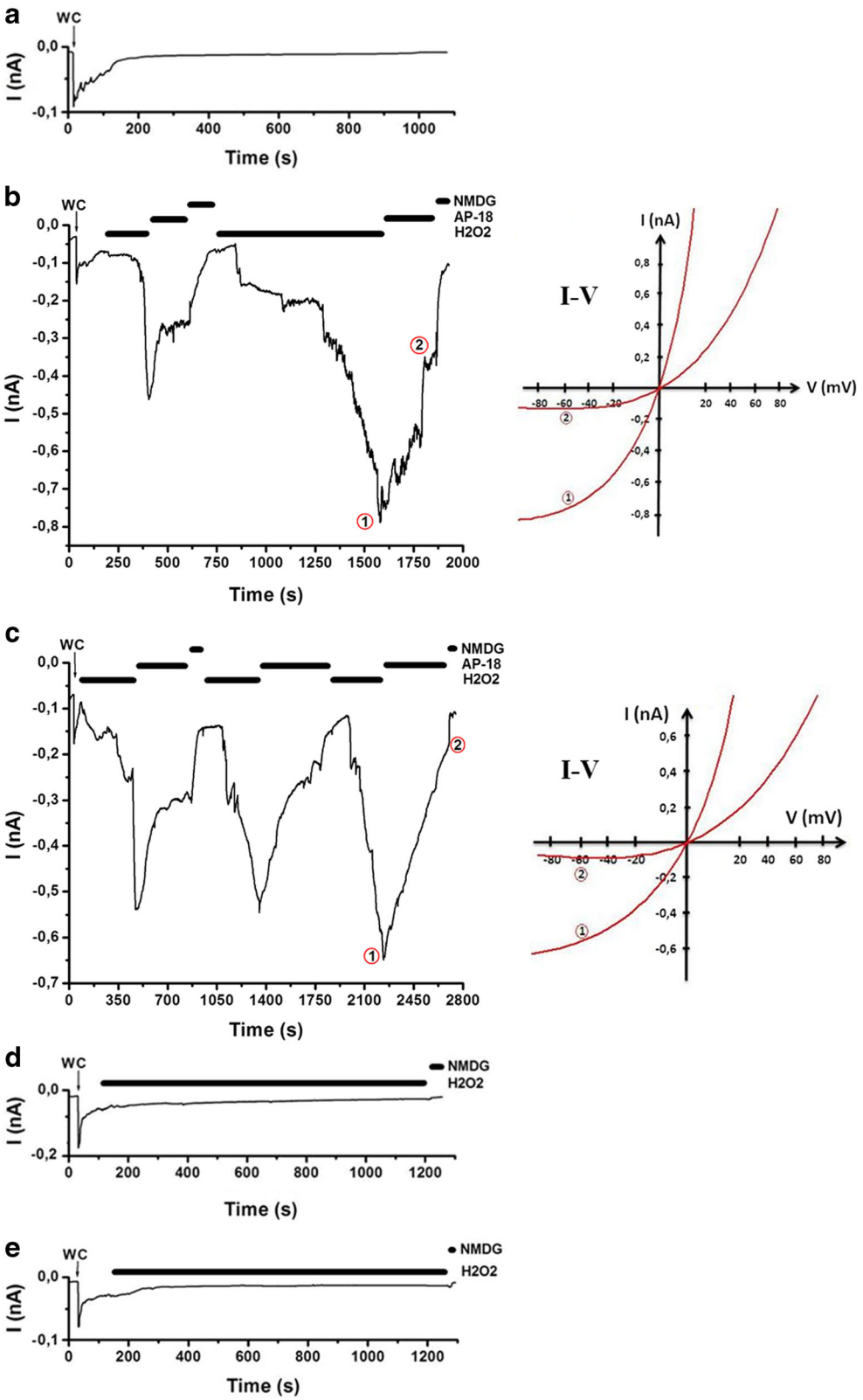

Fig. 7 Effects of E2, TMX, and RLX treatments on TRPA1 in the DRG of control and OVX rats. The holding potential was −60 mV. **a** Control: Records from the control neuron without stimulation of H_2O_2. **b** Control+H_2O_2 group: DRG was isolated from control rats without ovariectomy induction, and then, they were stimulated by H_2O_2 but inhibited by AP18 (0.020 mM). **c** OVX+H_2O_2 group: TRPA1 currents in the DRG neurons of OVX rats were gated by H_2O_2 but inhibited by AP18. **d** OVX+E2 group: The rats received E2 (80 μg/kg) for 14 days after ovariectomy, and then, the DRG neurons were stimulated by H_2O_2 but inhibited by AP18. **e** OVX+TMX group: After treatment of subcutaneous TMX (1 mg/kg) for 14 days in OVX rats, the DRG was stimulated by H_2O_2. **f** OVX+RLX group: After treatment of subcutaneous RLX (1 mg/kg) for 14 days in OVX rats, the DRG was stimulated by H_2O_2. *WC* whole cell

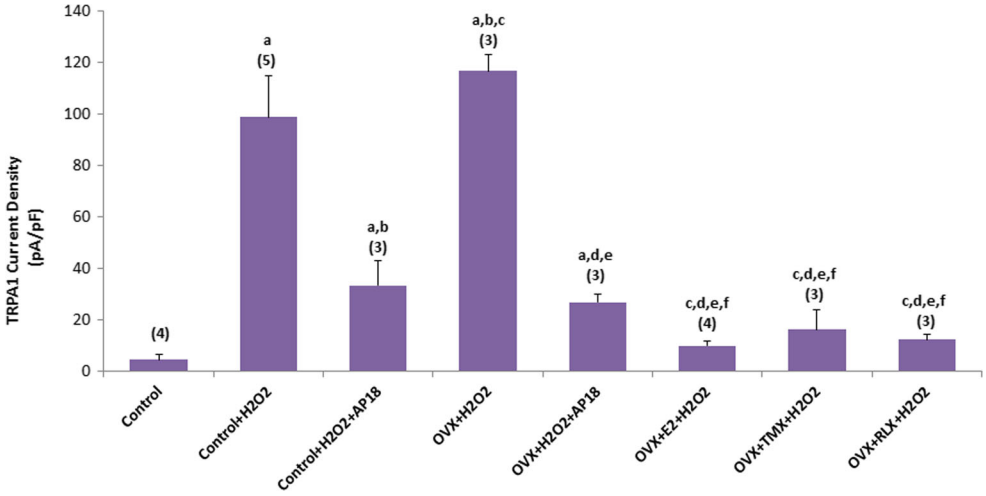

Fig. 8 Protective roles of E2, TMX, and RLX treatments on TRPA1 capacitances of the DRG in control and OVX rats. Except for control records, TRPA1 currents in the DRG neurons of rats were gated by H_2O_2 (10 mM) in the patch chamber, and they were inhibited by AP18 (0.02 mM) in the bath of the patch chamber. *N* numbers of the groups were indicated in parentheses ($^{a}p < 0.001$ versus control, $^{b}p < 0.05$ and $^{d}p < 0.001$ versus control+H_2O_2 group, $^{c}p < 0.001$ versus control+H_2O_2+AP18 group, $^{e}p < 0.001$ versus OVX+H_2O_2 group, $^{f}p < 0.001$ versus OVX+H2O2+AP18 group)

(15.19 pA/pF) and OVX+H_2O_2+ACA (11.08 pA/pF) groups by ACA treatments (Fig. 4). OVX-induced TRPM2 activities were also fully blocked in the OVX+E2, OVX+TMX, and OVX+RLX groups by E2, TMX, and RLX treatments, and the mean densities were markedly ($p < 0.001$) lower in the OVX+E2+H_2O_2 (6.76 pA/pF), OVX+TMX+H_2O_2 (4.22 pA/

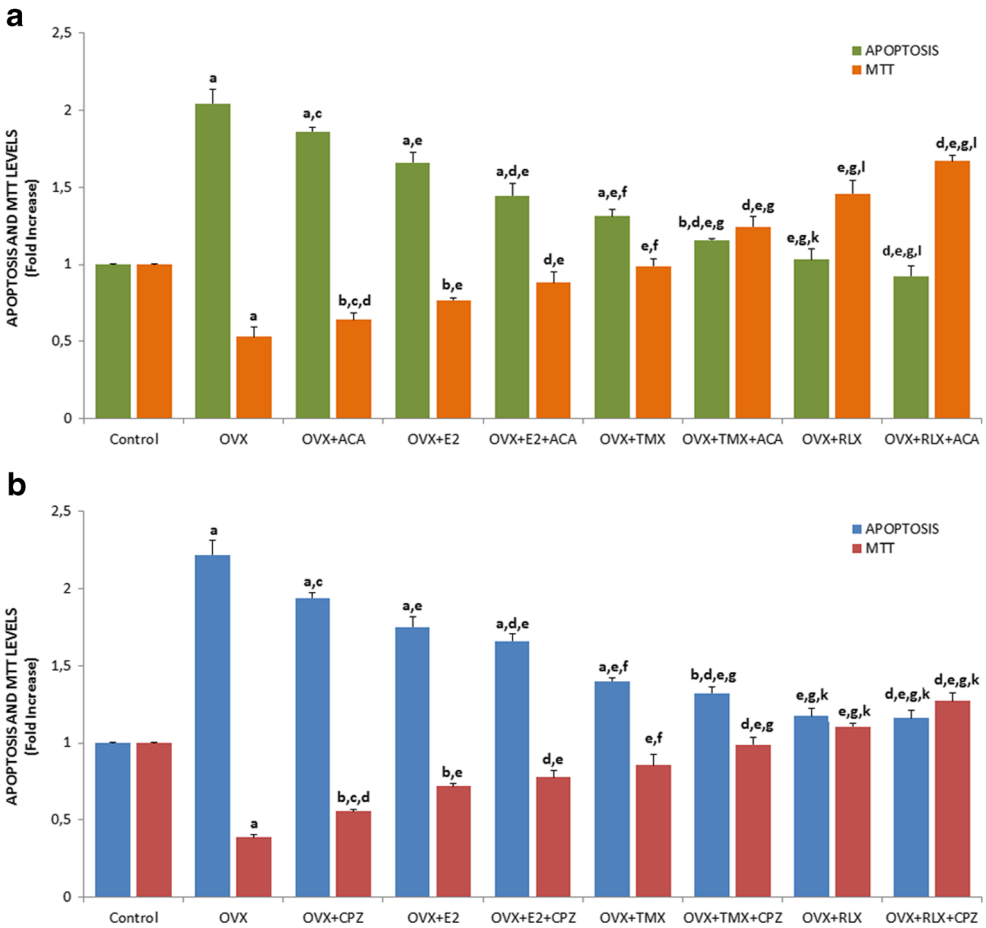

Fig. 9 Protective roles of E2, TMX, and RLX treatments in apoptosis and MTT levels through TRPM2 (**a**) and TRPV1 (**b**) in the HPC neurons of OVX rats [mean ± SD and $n = 12$ except control ($n = 8$)]. The HPC neurons were stimulated in vitro with CHPx (1 mM) (Fig. 7a) and capsaicin (0.01 mM) (Fig. 7b), although they were inhibited by ACA (0.025 mM) and CPZ (0.1 mM). Values were expressed as fold increase over the pretreatment level (experimental/control) ($^{a}p < 0.001$ and $^{b}p < 0.05$ versus control; $^{c}p < 0.05$ and $^{e}p < 0.001$ versus OVX group; $^{d}p < 0.05$ versus ACA and CPZ groups in OVX, OVX+E2, OVX+TMX, and OVX+RLX groups; $^{f}p < 0.05$ and $^{g}p < 0.001$ versus OVX+E2 group; $^{k}p < 0.05$ versus OVX+TMX group)

pF), and OVX+RLX+H_2O_2 (3.98 pA/pF) groups than in the control+H_2O_2, control+H_2O_2+ACA, OVX+H_2O_2, and OVX+H_2O_2+ACA groups.

The Protective Roles of E2, TMX, and RLX Treatments on TRPV1 Capacitances in the DRG of OVX Rats

Figures 5 and 6 indicate the protective effects of E2, TMX, and RLX treatments on TRPV1 activity in the DRG of OVX rats. CAP (0.01 mM) induced a current in native DRG neurons (Fig. 5b). Reaching amplitudes of well above 0.55 nA, the currents induced by CAP further developed gradually (between 0.4 and 1.2 min) following the addition of CAP to the patch chamber medium although they were blocked by CPZ and $NMDG^+$ (see Fig. 5b, c). The mean values of the current densities of the DRG neurons were markedly ($p < 0.001$) higher in the control+CAP (65.36 pA/pF) and OVX+CAP (155.29 pA/pF) groups than in the control group (3.12 pA/pF). In comparison to the control+CAP group, the densities were further increased in the OVX+CAP group by ovariectomy induction. However, the mean current densities were decreased to control levels in the control+CAP+CPZ (12.67 pA/pF) and OVX+CAP+CPZ (20.90 pA/pF) groups by CPZ treatments (Fig. 6). OVX-induced TRPV1 activities are also fully blocked in the OVX+E2, OVX+TMX, and OVX+RLX groups by E2, TMX, and RLX treatments, and the mean densities were markedly ($p < 0.001$) lower in the OVX+E2+CAP (15.06 pA/pF), OVX+TMX+CAP (3.39 pA/pF), and OVX+RLX+CAP (3.00 pA/pF) groups than in the control+CAP and OVX+CAP groups.

The Protective Roles of E2, TMX, and RLX Treatments on TRPA1 Capacitances in the DRG of OVX Rats

The protective effects of E2, TMX, and RLX treatments on TRPA1 activity in the DRG of OVX rats are shown in Figs. 7 and 8. TRPA1 currents were induced in the DRG neurons by H_2O_2 (Fig. 7b). Reaching amplitudes of the currents were above 0.75 nA. These currents were reversibly and partially blocked by AP18 (0.02 mM) and $NMDG^+$ (see Fig. 7b, c). There was no current in the absence of H_2O_2 in the DRG of control animals as those used for studying TRPA1. The mean values of the current densities of the DRG neurons were significantly ($p < 0.001$) higher in the control+H_2O_2 (98.79 pA/pF) and OVX+H_2O_2 (116.45 pA/pF) groups than in the control group (4.45 pA/pF). In comparison to the control+H_2O_2

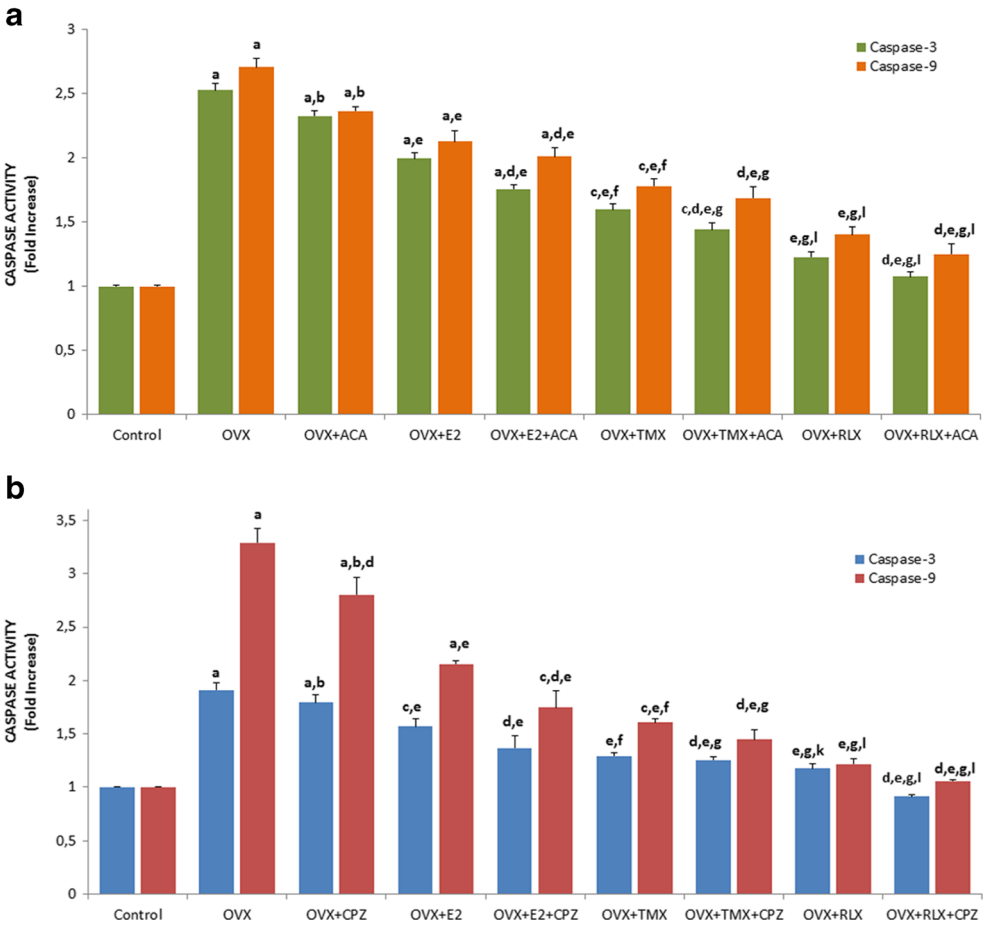

Fig. 10 Protective roles of E2, TMX, and RLX treatments in caspase-3 and caspase-9 activities through TRPM2 (**a**) and TRPV1 (**b**) in HPC neurons of OVX rats [mean ± SD and $n = 12$ except control ($n = 8$)]. The HPC neurons were stimulated in vitro with CHPx (1 mM) (**a**) and capsaicin (0.01 mM) (**b**), although they were inhibited by ACA (0.025 mM) and CPZ (0.1 mM) ($^a p < 0.001$ and $^c p < 0.05$ versus control; $^b p < 0.05$ and $^e p < 0.001$ versus OVX group; $^d p < 0.05$ versus ACA and CPZ groups in OVX, OVX+E2, OVX+TMX, and OVX+RLX groups; $^f p < 0.05$ and $^g p < 0.001$ versus OVX+E2 group; $^k p < 0.05$ versus OVX+TMX group)

group, the densities were further increased in the OVX+H_2O_2 group by ovariectomy induction ($p < 0.05$). However, the mean current densities were decreased to control levels in the control+H_2O_2+AP18 (26.77 pA/pF) and OVX+H_2O_2+AP18 (20.90 pA/pF) groups by CPZ treatments (Fig. 8). OVX-induced TRPA1 activities are also fully blocked in the OVX+E2 (Fig. 7d), OVX+TMX (Fig. 7e), and OVX+RLX (Fig. 7f) groups by E2, TMX, and RLX treatments, and the mean densities were significantly ($p < 0.001$) lower in the OVX+E2+H_2O_2 (9.91 pA/pF), OVX+TMX+H_2O_2 (16.23 pA/pF), and OVX+RLX+H_2O_2 (12.25 pA/pF) groups than in the control+H_2O_2 and OVX+H_2O_2 groups.

Results of Apoptosis, MTT, and Caspase-3 and Caspase-9 Values in the HPC Neurons of OVX Rats

Figures 9 and 10 show the effects of DEX on ovariectomy-induced apoptosis, cell viability (MTT) levels, and caspase-3 and caspase-9 activities through TRPM2 (Figs. 9a and 10a) and TRPV1 (Figs. 9b and 10b) activation in the HPC neurons. The apoptosis levels ($p < 0.001$) and the caspase-3 and caspase-9 activities were markedly higher in the OVX groups than in the control group, although the MTT levels were markedly ($p < 0.001$) lower in the OVX group than in the control group. The apoptosis levels ($p < 0.001$) and caspase-3 and caspase-9 activities were decreased by E2, TMX, and RLX treatments, and they were significantly ($p < 0.001$) lower in the OVX+E2, OVX+TMX, and OVX+RLX groups than in the OVX treatment groups, although MTT levels were markedly ($p < 0.001$) increased in the groups by OVX treatments. The apoptosis levels and caspase-3 and caspase-9 activities were further decreased in the OVX, OVX+E2, OVX+TMX, and OVX+RLX by TRPM2 antagonist (ACA) and TRPV1 antagonist (CPZ) treatments ($p < 0.05$), whereas the MTT levels were increased in the groups by both treatments ($p < 0.05$). The protective role of E2, TMX, and RLX were also observed on apoptosis, cell viability levels, and caspase-3 and caspase-9 activities through TRPM2 and TRPV1 activation in the HPC neurons (data are not shown).

Results of Mitochondrial Membrane Depolarization (JC-1) and Cytosolic OFR Production in HPC Neurons of OVX Rats

We investigated the protective effects of DEX on OFR and JC-1 levels in the HPC neurons through TRPM2 (Fig. 11a) and TRPV1 (Fig. 11b). The OFR and JC-1 levels in the HPC neurons were markedly ($p < 0.05$ and $p < 0.001$) higher in the

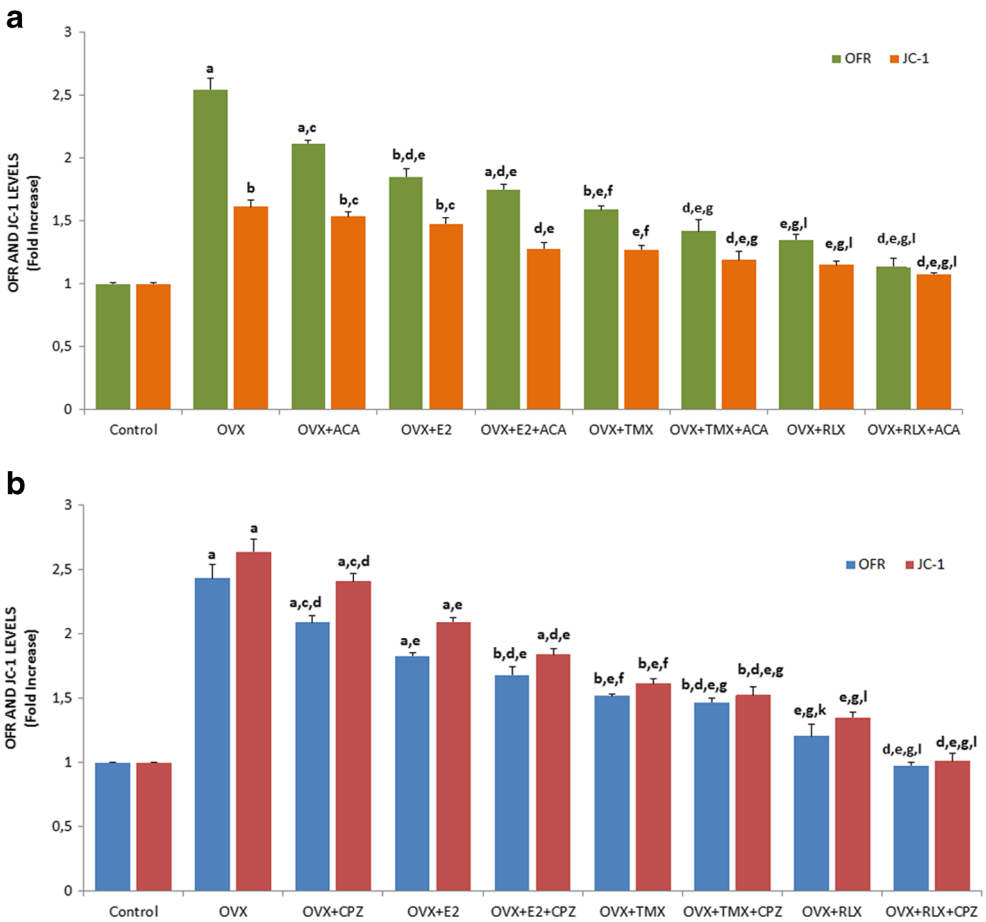

Fig. 11 Effects of E2, TMX, and RLX treatments on cytosolic oxygen free radical (OFR) production and mitochondrial membrane depolarization (JC-1) levels through TRPM2 and TRPV1 in HPC neurons of OVX rats [mean ± SD and $n = 12$ except control ($n = 8$)]. The HPC neurons were stimulated in vitro with CHPx (1 mM) (Fig. 9a) and capsaicin (0.01 mM) (Fig. 9b), although they were inhibited by ACA (0.025 mM) and CPZ (0.1 mM) ($^{a}p < 0.001$ and $^{b}p < 0.05$ versus control; $^{c}p < 0.05$ and $^{e}p < 0.001$ versus OVX group; $^{d}p < 0.05$ versus ACA and CPZ groups in OVX, OVX+E2, OVX+TMX, and OVX+RLX groups; $^{f}p < 0.05$ and $^{g}p < 0.001$ versus OVX+E2 group; $^{k}p < 0.05$ versus OVX+TMX group)

OVX groups than in the control group. The OFR and JC-1 levels were markedly ($p < 0.001$) lower in the OVX+E2, OVX+TMX, and OVX+RLX groups than in the OVX treatment groups. In addition, the OFR and JC-1 levels were further decreased in the OVX, OVX+E2, OVX+TMX, and OVX+RLX groups by ACA and CPZ treatments ($p < 0.05$). The OFR and JC-1 levels were markedly ($p < 0.05$) lower in the OVX+RLX group than in the OVX+TMX group.

Results of PARP and Procaspase-3 and Procaspase-9 Expression in DRG and HPC Neurons

In the mitochondrial apoptotic cascade, caspase-3 and caspase-9 activities are important indicators in cells [2, 33]. Active caspase-3 and caspase-9 are produced by further processing of procaspase-3 and procaspase-9, respectively [34]. Procaspase-3 and procaspase-9 as indicators of apoptosis were assayed in the DRG (Fig. 12a) and the hippocampus (Fig. 12b). The expression levels of procaspase-3 and procaspase-9 in the DRG and the hippocampus were markedly ($p < 0.05$) lower in the OVX group than in the control group, although they were markedly ($p < 0.05$) higher in the OVX+E2, OVX+TMX, and OVX+RLX groups than in the OVX-only group. The procaspase-3 and procaspase-9 expression levels in the HPC neurons were further increased in the OVX+RLX group in comparison to the control group.

TRPM2 is activated by PARP-induced ADPR production. PARP expression levels in DRG and HPC neurons are shown in Fig. 13a, b, respectively. The PARP expression levels in the HPC neurons were markedly ($p < 0.05$) higher in the OVX group than in the control group. However, PARP expression levels in the HPC neurons were significantly ($p < 0.05$) lower in the OVX+E2, OVX+TMX, and OVX+RLX groups than in the OVX-only group. The PARP expression level in the HPC neurons was further increased in the OVX+RLX group in comparison to the control group. There was no statistical

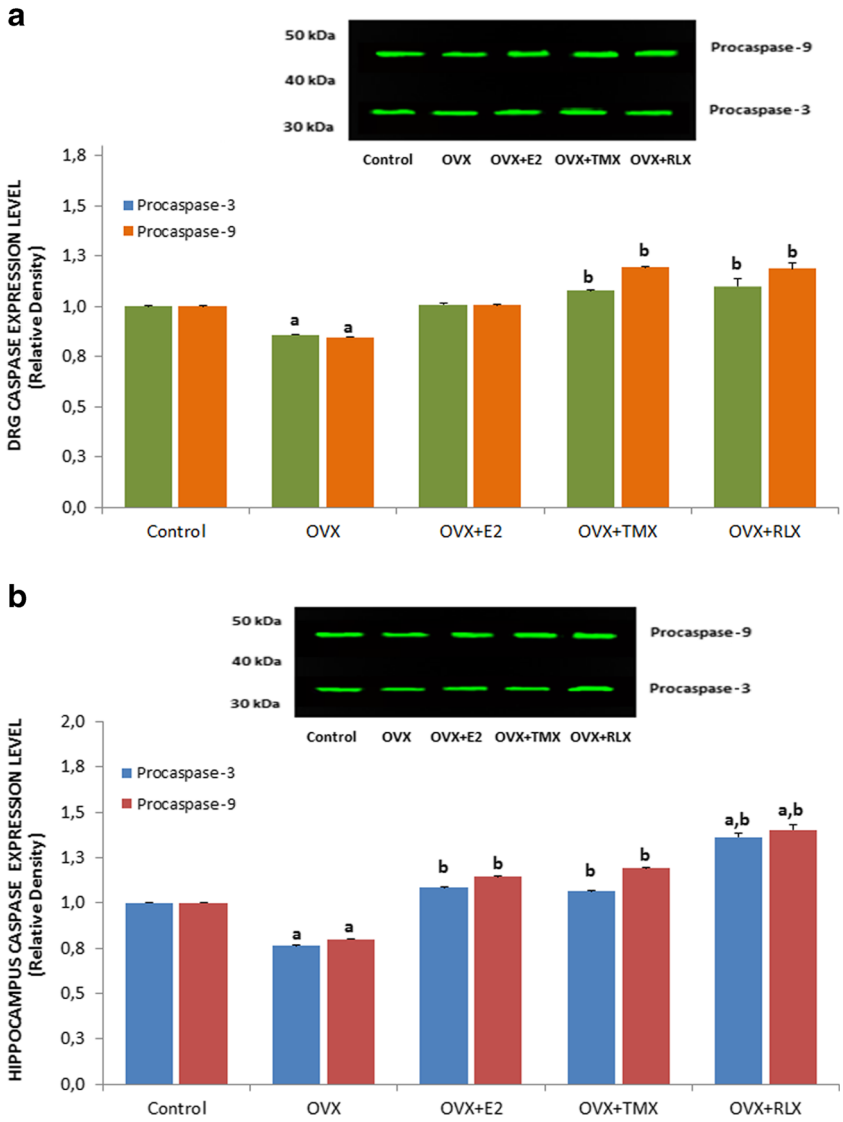

Fig. 12 Roles of E2, TMX, and RLX treatments on procaspase-3 and procaspase-9 expression levels in DRG (Fig. 10a) and HPC (Fig. 10b) neurons of OVX rats. Values are presented as mean ± SD of three separate experiments and expressed relative density (fold increase) ($^{a}p < 0.05$ versus control, $^{b}p < 0.05$ versus OVX group)

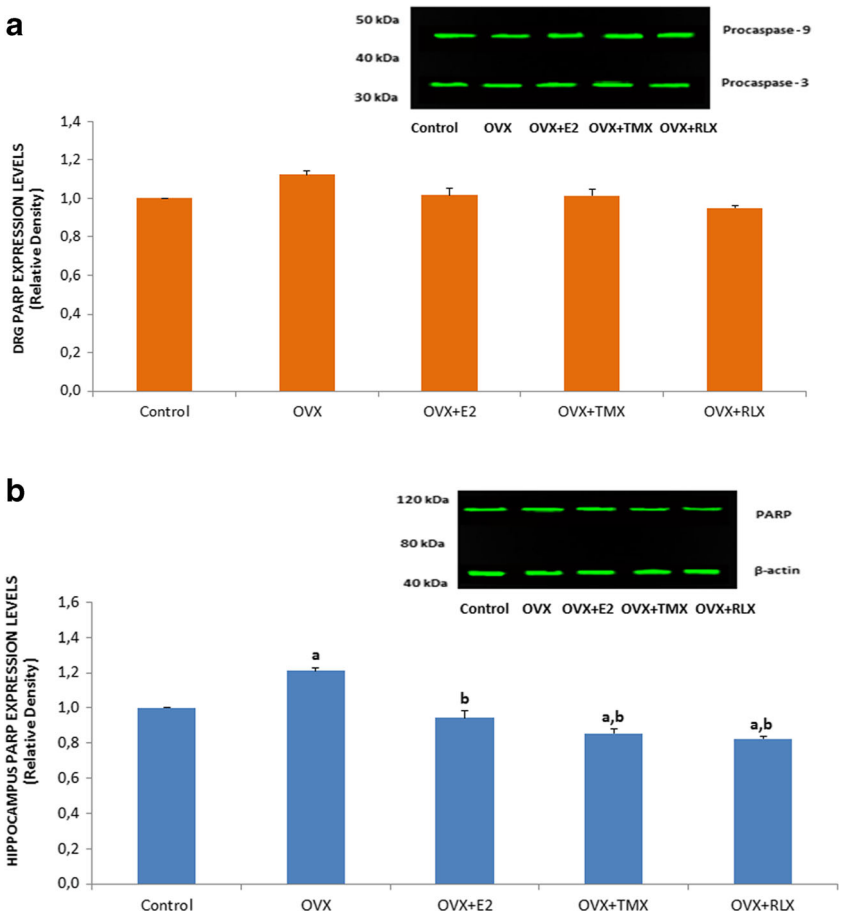

Fig. 13 Roles of E2, TMX, and RLX treatments on TRPM2 and TRPV1 expression levels in DRG (**a**) and HPC (**b**) neurons of OVX rats. Values are presented as mean ± SD of three separate experiments and expressed relative density (fold increase) ([a]$p < 0.05$ versus control, [b]$p < 0.05$ versus OVX group)

difference in terms of DRG PARP expression levels among the five groups.

Results of TRPM2 and TRPV1 Expression Levels in DRG and HPC Neurons

TRPM2 and TRPV1 expression levels in the DRG and hippocampus are shown in Fig. 14a, b, respectively. Expression levels of TRPM2 and TRPV1 in the DRG and hippocampus were markedly ($p < 0.05$) higher in the OVX group than in the control group, although they were markedly ($p < 0.05$) lower in the OVX+E2, OVX+TMX, and OVX+RLX groups than in the OVX only group. The procaspase-3 and procaspase-9 expression levels in the HPC neurons were further decreased in the OVX+RLX group in comparison to the OVX group.

Discussion

Relative estrogen deprivation in postmenopausal women is associated with increased levels of oxidative stress and apoptosis, and it increases the risk of certain diseases, including degenerative processes in the central nervous system [35]. It has been reported that oxidative stress increases in female rat brains after ovariectomy [36] and that E2 protects the hippocampus, cerebral cortex, and hypothalamus from mitochondrial oxidative stress [21, 28]. E2 protects neurons against overload Ca^{2+} influx via modulation of L-type VGCC [37]. TMX and RLX are SERM modulator drugs in postmenopausal women. In addition to their effectiveness as anticancer and bone loss modulators, they have been reported to play a regulator role in VGCC activation and mitochondrial OFR production in neurons [21, 28]. Excessive production of mitochondrial OFR with an overload of Ca^{2+} influx through TRPA1, TRPM2, and TRPV1 activity is one of the main causes of neurodegenerative diseases and pain [8, 11, 12, 16]. The aim of this study was to evaluate whether E2, TMX, and RLX functionally interact with TRPA1, TRPM2, and TRPV1 in the HPC and DRG neurons of OVX rats. Our data suggest that E2, TMX, and RLX are potent inhibitors of TRPA1, TRPM2, and TRPV1 in these neurons. We suggest that E2, TMX, and RLX-dependent alterations of Ca^{2+} influx through the TRPA1, TRPM2, and TRPV1 are responsible on pathophysiological mechanisms in ovariectomy-induced HPC oxidative injury and pain induction.

TRPM2 activity is gated by oxidative stress level [3]. The production of ADPR from DNA-damaged nuclei is increased by excessive production of OFRs through stimulation of

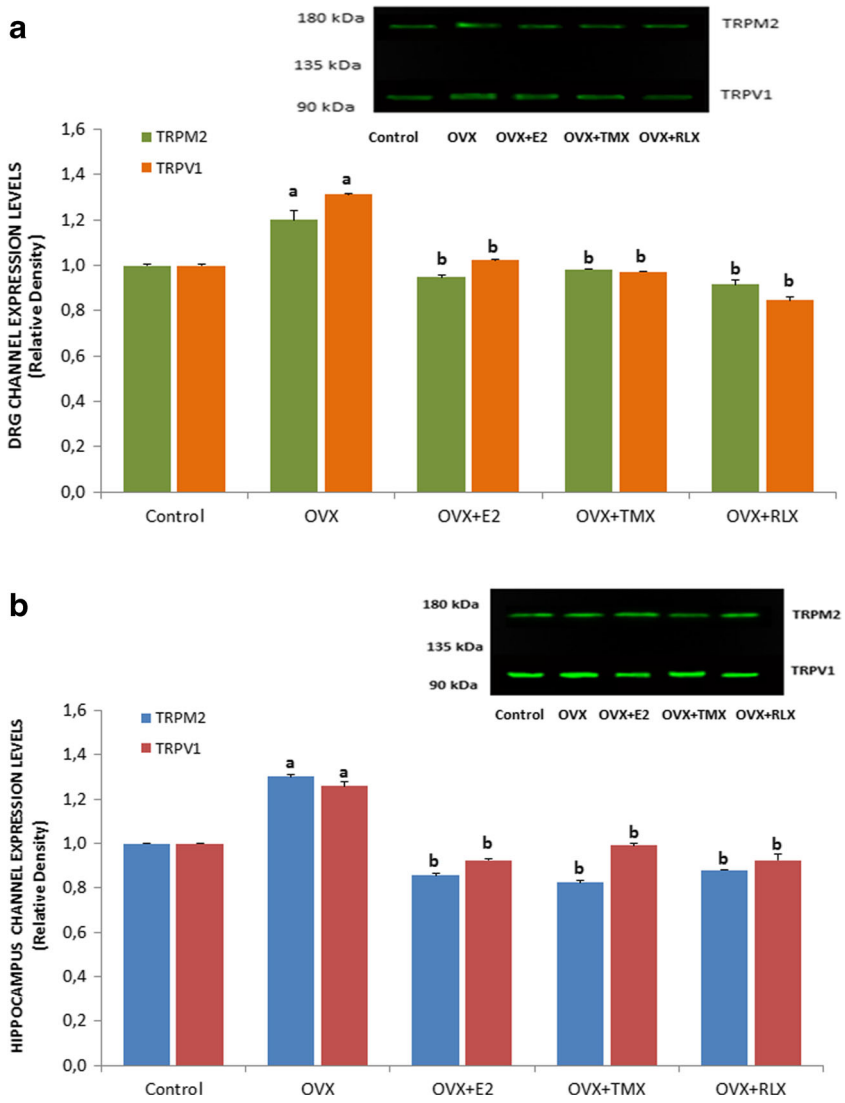

Fig. 14 Effects of E2, TMX, and RLX treatments on TRPM2 and TRPV1 expression levels in DRG (**a**) and HPC (**b**) neurons of OVX rats. Values are presented as mean ± SD of three separate experiments and expressed relative density (fold increase) ($^{a}p < 0.05$ versus control, $^{b}p < 0.05$ versus OVX group)

oxidative stress redox systems induced [1]. The H_2O_2 binds to the TRPM2 C terminal NUDT9-H domain for activation of TRPM2 [3, 4]. Expression level of TRPM2 is high in the hippocampus and the DRG [15], a subset of neurons that are mainly susceptible to oxidative stress-induced damage in neurodegenerative disease and pain [1, 6]. E2, TMX, and RLX are lipophilic antioxidants, and they reduce excessive production of mitochondrial oxidative stress via the regulation of MPT function [20, 24]. In the current study, we observed increased levels of TRPM2 current density, apoptosis, and mitochondrial OFR levels via ovariectomy induction in the DRG and hippocampus, although the densities, apoptosis, and oxidative stress levels in the neurons were decreased by E2, RLX, and TMX treatments. Hence, ovariectomy through TRPM2 activity participated to cell death in response to overload Ca^{2+} influx and excessive mitochondrial oxidative stress, although the channel activity and apoptosis levels were decreased by E2, TMX, and RLX treatments through inhibition of mitochondrial oxidative stress.

E2 is a steroid hormone, and there is a functional interconnection between TRP channels and steroid hormones. For example, the expression of steroid receptors is increased in prostate LNCaP cell lines by the TRPV1 agonist CAP [37]. Steroids and chronic stress also increased TRPV1 expression in DRG neurons [38]. Steroids can activate TRP channels in the DRG neurons of OVX rats by direct binding [39], although the molecular mechanisms have not been clarified in the DRG neurons. DRG neurons have an important modulator role in peripheral pain and spinal cord injury-induced pathways [12]. In addition to the anticancer and antioxidant effects of E2 and TMX, they also play an important role in the control of oxidative brain injury [19, 20] and pain modulation [27]. Recently, modulator role of E2 through subcutaneously injected TRPA1 was reported in oxaliplatin-induced peripheral neuropathy [40]. In the current study, we observed a modulator role of steroid E2, TMX, and RLX on mitochondrial membrane depolarization, channel expression, and Ca^{2+} influx via TRPA1, TRPM2, and TRPV1 in the DRG neurons.

It is well known that the mitochondrial membrane potential via the conversion of ADP to ATP via ATP synthase is important in oxidative phosphorylation [20]. Similar to the current results, ATP-induced increase of $[Ca^{2+}]_i$ concentration and calcium currents in the DRG neurons are decreased by E2 treatment [41, 42]. Inhibition of TRPV1 activation was also reported by long-term exposure of DRG neurons to E2 [5]. It was also reported that CAP-induced TRPV1 currents were decreased in the nociceptive neurons of adult rats by E2 treatment [43]. On the other hand, increased allodynia and HPC TRPV1 activity in rats with inflammatory temporomandibular joints have been reported in OVX-treated rats [10].

Mitochondria play an important role in initiating apoptosis. Elevated MPT and Ca^{2+} accumulation induce mitochondrial membrane depolarization through the swelling and rupture of mitochondrial membranes [2, 33], and it activates the caspase cascade and apoptotic pathways in the hippocampus and the DRG [11, 12]. TMX and RLX are lipophilic membrane-permeable antioxidants and calcium channel regulators that overload Ca^{2+} accumulation-induced MPT, which is inhibited by TMX [44]. The TRPM2 and TRPV1 results of the current study indicate that the blockade of Ca^{2+} uptake into mitochondria with E2, TMX, and RLX—as well as increases in Ca^{2+} influx resulting in increased $[Ca^{2+}]_i$ concentration—were able to decrease mitochondrial membrane depolarization, excessive OFR production, and apoptosis mediated by TRPM2 agonist (CHPx) and TRPV1 agonist (CAP).

Several pathophysiological mechanisms of caspase activities and apoptosis are regulated by $[Ca^{2+}]_i$ concentration [45]. Cell proliferation is increased by a modest increase in $[Ca^{2+}]_i$, although the release of proapoptotic factors through increased mitochondrial Ca^{2+} is increased by overload Ca^{2+} influx [2, 33]. In addition to VGCC and chemical channels, several TRP channels have been proposed to be involved in the H_2O_2-mediated $[Ca^{2+}]_i$ increase, including the TRPM2 and TRPV1. Oxidative stress-induced cell apoptosis through activation of TRPM2 and TRPV1 has been implicated in DRG and HPC [11, 12]. Oxidative stress and CAP-induced apoptosis, cell viability, and caspase-3 and caspase-9 values were decreased by E2, TMX, and RLX treatments through reduced activity of TRPM2 and TRPV1 in the DRG and the HPC neurons. Similarly, incubation-induced apoptosis in retinal cells was reportedly reduced by E2 treatment [46]. In addition, the protective role of E2 through modulation of Ca^{2+} influx and VGCC on H_2O_2-induced apoptosis in primary cultural rat retinal cells has been reported [47]. To our knowledge, there are no reports on the regulation of apoptosis, cell viability, or caspase-3 and caspase-9 values in TRP channels, except TRPV5. E2 has been shown to be involved in the modulation of Ca^{2+} influx in rat renal cells via TRPV5 [48].

In conclusion, the current study revealed involvement of Ca^{2+} influx through TRPA1, TRPM2, and TRPV1 on ovariectomy-induced mitochondrial oxygen free radical production, apoptosis, and channel expression levels in the DRG and HPC neurons of OVX rats by E2, TMX, and RLX. These findings suggest that TRPM2 and TRPV1 may first time play an important role in neurological diseases and peripheral pain associated with ovariectomy and oxidative stress, although TMX and RLX treatments may account for their neuroprotective activity against apoptosis, oxidative stress, and Ca^{2+} influx. Their inhibitory effects on ovariectomy-induced gating TRPA1, TRPM2, and TRPV1 should be considered as potential pharmacological agents for treating ovariectomy-mediated activation of pain receptors and of mitochondrial oxidative brain injuries.

Acknowledgments The abstracts of the study were presented at the 6th World Congress of Oxidative Stress, Calcium Signaling and TRP Channels, held on 24 and 27 May 2016 in Isparta, Turkey (www.cmos.org.tr). The authors wish to thank the researcher technicians İshak Suat Övey and Muhammet Şahin (Neuroscience Research Center, SDU, Isparta, Turkey) for helping with the Western blot and plate reader analyses.

Authorship Contributions MN formulated the hypothesis and was responsible for writing the report. Ovariectomy of rats was performed by MN. The analyses were performed by YY.

Compliance with Ethical Standards

Funding Unit of Scientific Research Project (BAP) of Suleyman Demirel University.

Financial Disclosure This study was partially supported by the Unit of Scientific Research Project (BAP) of Suleyman Demirel University in Isparta, Turkey (Project Number BAP: 4135-YL2-14). There is no financial disclosure for the current study.

Conflict of Interest The authors declare that they have no conflict of interest.

References

1. Nazıroğlu M (2007) New molecular mechanisms on the activation of TRPM2 channels by oxidative stress and ADP-ribose. Neurochem Res 32:1990–2001
2. Espino J, Bejarano I, Redondo PC, Rosado JA, Barriga C, Reiter RJ, Pariente JA, Rodríguez AB (2010) Melatonin reduces apoptosis induced by calcium signaling in human leukocytes: evidence for the involvement of mitochondria and Bax activation. J Membr Biol 233:105–118
3. Hara Y, Wakamori M, Ishii M, Maeno E, Nishida M, Yoshida T, Yamada H, Shimizu S et al (2002) LTRPC2 Ca2+-permeable channel activated by changes in redox status confers susceptibility to cell death. Mol Cell 9:163–173
4. Nazıroğlu M, Lückhoff A (2008) A calcium influx pathway regulated separately by oxidative stress and ADP-ribose in TRPM2 channels: single channel events. Neurochem Res 33:1256–1262

5. Caterina MJ, Schumacher MA, Tominaga M, Rosen TA, Levine JD, Julius D (1997) The capsaicin receptor: a heat-activated ion channel in the pain pathway. Nature 1997(389):816–824
6. Nazıroğlu M (2015) TRPV1 channel: a potential drug target for treating epilepsy. Curr Neuropharmacol 13:239–247
7. Pecze L, Jósvay K, Blum W, Petrovics G, Vizler C, Oláh Z, Schwaller B (2016) Activation of endogenous TRPV1 fails to induce overstimulation-based cytotoxicity in breast and prostate cancer cells but not in pain-sensing neurons. Biochim Biophys Acta 1863:2054–2064
8. Takahashi N, Kuwaki T, Kiyonaka S, Numata T, Kozai D, Mizuno Y, Yamamoto S, Naito S et al (2011) TRPA1 underlies a sensing mechanism for O2. Nat Chem Biol 7(10):701–711
9. Toda T, Yamamoto S, Yonezawa R, Mori Y, Shimizu S (2016) Inhibitory effects of Tyrphostin AG-related compounds on oxidative stress-sensitive transient receptor potential channel activation. Eur J Pharmacol 786:19–28
10. Wu YW, Bi YP, Kou XX, Xu W, Ma LQ, Wang KW, Gan YH, Ma XC (2010) 17-Beta-estradiol enhanced allodynia of inflammatory temporomandibular joint through upregulation of hippocampal TRPV1 in ovariectomized rats. J Neurosci 30:8710–8719
11. Kahya MC, Nazıroğlu M, Çiğ B. (2016) Modulation of diabetes-induced oxidative stress, apoptosis, and Ca2+ entry through TRPM2 and TRPV1 channels in dorsal root ganglion and hippocampus of diabetic rats by melatonin and selenium. Mol Neurobiol. 2016 [Epub ahead of print]. doi:10.1007/s12035-016-9727-3.
12. Özdemir ÜS, Nazıroğlu M, Şenol N, Ghazizadeh V (2016) *Hypericum perforatum* attenuates spinal cord injury-induced oxidative stress and apoptosis in the dorsal root ganglion of rats: involvement of TRPM2 and TRPV1 channels. Mol Neurobiol 53: 3540–3551
13. Obata K, Katsura H, Mizushima T, Yamanaka H, Kobayashi K, Dai Y, Fukuoka T, Tokunaga A et al (2005) TRPA1 induced in sensory neurons contributes to cold hyperalgesia after inflammation and nerve injury. J Clin Invest 115:2393–2401
14. Cristino L, de Petrocellis L, Pryce G, Baker D, Guglielmotti V, Di Marzo V (2006) Immunohistochemical localization of cannabinoid type 1 and vanilloid transient receptor potential vanilloid type 1 receptors in the mouse brain. Neuroscience 139:1405–1415
15. Fonfria E, Murdock PR, Cusdin FS, Benham CD, Kelsell RE, McNulty S (2006) Tissue distribution profiles of the human TRPM cation channel family. J Recept Signal Transduct Res 26: 159–178
16. Bai JZ, Lipski J (2010) Differential expression of TRPM2 and TRPV4 channels and their potential role in oxidative stress-induced cell death in organotypic hippocampal culture. Neurotoxicology 31:204–214
17. Nativi C, Gualdani R, Dragoni E, Di Cesare ML, Sostegni S, Norcini M, Gabrielli G, la Marca G et al (2013) A TRPA1 antagonist reverts oxaliplatin-induced neuropathic pain. Sci Rep 3:2005
18. Cho T, Chaban VV (2012) Expression of P2X3 and TRPV1 receptors in primary sensory neurons from estrogen receptors-α and estrogen receptor-β knockout mice. Neuroreport 23:530–534
19. Kimelberg HK, Jin Y, Charniga C, Feustel PJ (2003) Neuroprotective activity of tamoxifen in permanent focal ischemia. J Neurosurg 99:138–142
20. Moreira PI, Custodio JB, Oliveira CR, Santos MS (2005) Brain mitochondrial injury induced by oxidative stress-related events is prevented by tamoxifen. Neuropharmacology 48:435–447
21. Osmanova S, Sezer E, Turan V, Zeybek B, Terek MC, Kanıt L (2011) The effects of raloxifene treatment on oxidative status in brain tissues and learning process of ovariectomized rats. Iran J Reprod Med 9:295–300
22. Ozgocmen S, Kaya H, Fadillioglu E, Yilmaz Z (2007) Effects of calcitonin, risedronate, and raloxifene on erythrocyte antioxidant enzyme activity, lipid peroxidation, and nitric oxide in postmenopausal osteoporosis. Arch Med Res 38:196e205
23. O'Neill K, Chen S, Brinton RD (2004) Impact of the selective estrogen receptor modulator, raloxifene, on neuronal survival and outgrowth following toxic insults associated with aging and Alzheimer's disease. Exp Neurol 185:63–80
24. Moreira PI, Custódio JB, Nunes E, Oliveira PJ, Moreno A, Seiça R, Oliveira CR, Santos MS (2011) Mitochondria from distinct tissues are differently affected by 17β-estradiol and tamoxifen. J Steroid Biochem Mol Biol 123:8–16
25. Huang Y, Lai B, Zheng P, Zhua YC, Yaoa T (2007) Raloxifene acutely reduces glutamate-induced intracellular calcium increase in cultured rat cortical neurons via inhibition of high-voltage-actıvated calcium current. Neuroscience 147:334–341
26. Dilek M, Nazıroğlu M, Oral BH, Övey İS, Küçükyaz M, Mungan MT, Kara HY, Sütçü R (2010) Melatonin modulates hippocampus NMDA receptors, blood and brain oxidative stress levels in ovariectomized rats. J Membr Biol 233:135–142
27. Kramer PR, Bellinger LL (2013) Modulation of temporomandibular joint nociception and inflammation in male rats after administering a physiological concentration of 17beta-oestradiol. Eur J Pain 17:174–184
28. Yazgan B, Yazgan Y, Övey İS (2016) Nazıroğlu M. Raloxifene and tamoxifen reduce PARP activity, cytokine and oxidative stress levels in the brain and blood of ovariectomized rats. J Mol Neurosci 60:214–222
29. Olah ME, Jackson MF, Li H, Perez Y, Sun HS, Kiyonaka S, Mori Y, Tymianski M et al (2009) Ca^{2+}-dependent induction of TRPM2 currents in hippocampal neurons. J Physiol 587(Pt 5):965–979
30. Grynkiewicz C, Poenie M, Tsien RY (1985) A new generation of Ca^{2+} indicators with greatly improved fluorescence properties. J Biol Chem 260:3440–3450
31. Espino J, Bejarano I, Paredes SD, Barriga C, Rodríguez AB, Pariente JA (2011) Protective effect of melatonin against human leukocyte apoptosis induced by intracellular calcium overload: relation with its antioxidant actions. J Pineal Res 51:195–206
32. Nazıroğlu M, Dikici DM, Dursun Ş (2012) Role of oxidative stress and Ca^{2+} signaling on molecular pathways of neuropathic pain in diabetes: focus on TRP channels. Neurochem Res 37:2065–2075
33. Nazıroğlu M (2015) Role of melatonin on calcium signaling and mitochondrial oxidative stress in epilepsy: focus on TRP channels. Tr J Biol 39:813–821
34. Li P, Nijhawan D, Budihardjo I, Srinivasula SM, Ahmad M, Alnemri ES, Wang X (1997) Cytochrome c and dATP-dependent formation of Apaf-1/caspase-9 complex initiates an apoptotic protease cascade. Cell 91:479–489
35. Phillips SM, Sherwin BB (1992) Effects on estrogen on memory function in surgically menopausal women. Psychoneuroendocrinology 17: 485–495
36. Vega-Vela NE, Osorio D, Avila-Rodriguez M, Gonzalez J, García-Segura LM, Echeverria V, Barreto GE (2016) L-type calcium channels modulation by estradiol. Mol Neurobiol [Epub ahead of print]. doi:10.1007/s12035-016-0045-6
37. Malagarie-Cazenave S, Olea-Herrero N, Vara D, Díaz-Laviada I (2009) Capsaicin, a component of red peppers, induces expression of androgen receptor via PI3K and MAPK pathways in prostate LNCaP cells. FEBS Lett 583:141–147
38. Zheng G, Hong S, Hayes JM, Wiley JW (2015) Chronic stress and peripheral pain: evidence for distinct, region-specific changes in visceral and somatosensory pain regulatory pathways. Exp Neurol 273:301–311
39. Scotland PE, Patil M, Belugin S, Henry MA, Goffin V, Hargreaves KM, Akopian AN (2011) Endogenous prolactin generated during peripheral inflammation contributes to thermal hyperalgesia. Eur J Neurosci 34:745–754

40. Pan Y, Huang S, Cai Z, Lan H, Tong Y, Yu X, Zhao G, Chen F (2016) TRPA1 and TRPM8 receptors may promote local vasodilation that aggravates oxaliplatin-induced peripheral neuropathy amenable to 17β-estradiol treatment. Curr Neurovasc Res 13:309-317
41. Lee DY, Chai YG, Lee EB, Kim KW, Nah SY, Oh TH, Rhim H (2002) 17β-estradiol inhibits high-voltage-activated calcium channel currents in rat sensory neurons via a non-genomic mechanism. Life Sci 70:2047–2059
42. Chaban VV, Mayer EA, Ennes HS, Micevych PE (2003) Estradiol inhibits ATP-induced intracellular calcium concentration increase in dorsal root ganglia neurons. Neuroscience 118:941–948
43. Xu S, Cheng Y, Keast JR, Osborne PB (2008) 17beta-estradiol activates estrogen receptor beta-signalling and inhibits transient receptor potential vanilloid receptor 1 activation by capsaicin in adult rat nociceptor neurons. Endocrinology 149:5540–5548
44. Cardoso CM, Almeida LM, Custódio JB (2004) Protection of tamoxifen against oxidation of mitochondrial thiols and NAD(P)H underlying the permeability transition induced by prooxidants. Chem Biol Interact 148:149–161
45. Kumar VS, Gopalakrishnan A, Nazıroğlu M, Rajanikant GK (2014) Calcium ion-the key player in cerebral ischemia. Curr Med Chem 21:2065–2075
46. Yu X, Rajala RV, McGinnis JF, Li F, Anderson RE, Yan X, Li S, Elias RV et al (2004) Involvement of insulin/phosphoinositide 3-kinase/Akt signal pathway in 17 beta-estradiol-mediated neuroprotection. J Biol Chem 26(279):13086–13094
47. Feng Y, Wang B, Du F, Li H, Wang S, Hu C, Zhu C, Yu X (2013) The involvement of PI3K-mediated and L-VGCC-gated transient Ca^{2+} influx in 17β-estradiol-mediated protection of retinal cells from H_2O_2-induced apoptosis with Ca^{2+} overload. PLoS One 8: e77218
48. Irnaten M, Blanchard-Gutton N, Praetorius J, Harvey BJ (2009) Rapid effects of 17 beta-estradiol on TRPV5 epithelial Ca^{2+} channels in rat renal cells. Steroids 74:642–649